Environmental Pollution 159 (2011) 1048–1057

Contents lists available at ScienceDirect

Environmental Pollution

journal homepage: www.elsevier.com/locate/envpol

Spatiotemporal dynamics of spring and stream water chemistry in a high-mountain area

Mirosław Żelazny [a], Aleksander Astel [b,*], Anna Wolanin [a], Stanisław Małek [c]

[a] Jagiellonian University, Institute of Geography and Spatial Management, Department of Hydrology, 7 Gronostajowa Str., 30-387 Cracow, Poland
[b] Environmental Chemistry Research Unit, Biology and Environmental Protection Institute, Pomeranian Academy, 22a Arciszewskiego Str., Słupsk, 76-200, Poland
[c] Department of Forest Ecology, Forest Faculty, Agricultural University of Cracow, 46 29 Listopada Ave., Cracow, 31-425, Poland

Spatiotemporal dynamics of spring and stream water chemistry in unique high-mountain area was evaluated by the self-organizing map technique.

ARTICLE INFO

Article history:
Received 4 November 2010
Accepted 21 November 2010

Keywords:
Tatra Mountains
Basin
Water chemical profile
Unsupervised classification
Self-organizing maps
Rock
Spruce stands

ABSTRACT

The present study deals with the application of the self-organizing map (SOM) technique in the exploration of spatiotemporal dynamics of spring and stream water samples collected in the Chochołowski Stream Basin located in the Tatra Mountains (Poland). The SOM-based classification helped to uncover relationships between physical and chemical parameters of water samples and factors determining the quality of water in the studied high-mountain area. In the upper part of the Chochołowski Stream Basin, located on the top of the crystalline core of the Tatras, concentrations of the majority of ionic substances were the lowest due to limited leaching. Significantly higher concentration of ionic substances was detected in spring and stream samples draining sedimentary rocks. The influence of karst-type springs on the quality of stream water was also demonstrated.

1. Introduction

Waters draining high mountain basins can serve as models of natural basin functioning. The chemical composition of water in high mountain springs and streams and changes therein are determined primarily by natural factors such as tectonics, geologic structure, land cover, and land use (Allan and Flecker, 1993). The monitoring of chemical, physical, and biological properties of water resources plays an important role in understanding biogeochemical cycles. This matter is of great importance, especially in the case of water bodies (springs, streams, lakes) located in mountain ecosystems, as they provide considerable amounts of surface water of high purity. Until now, there have been only a few studies specified addressing water bodies in the Tatra Mountain ecosystem. Advanced water research in the Tatra Mountains usually dealt differences in water chemistry in springs, surface waters, and lakes. In the 1950s, one study was carried out on about 800 spring, surface, and lake water samples (Oleksynowa and Komornicki, 1960; Oleksynowa, 1970). A hydrochemical map was then produced and published in the Tatra National Park Atlas (scale: 1:50,000) (Trafas, 1985). Kopáček et al. (2004) correlated chemical and biochemical characteristics of alpine soils in the Tatra Mountains with lake water quality. Stuchlík et al. (2006) explored the chemical composition of Tatra Mountain lakes based on their response to acidification, while Křeček et al. (2006) analyzed hydrological processes in small catchments. However, none of these studies dealt with a complex analysis of the quality of water via the use of chemometric expertise. The quality of water depends on many factors and this is why a number of researchers have attempted to study it in various ecosystems using principal component analysis (Stanimirova et al., 2007), linear discriminant analysis (Astel et al., 2009), and classification tools (Astel et al., 2006). Although self-organizing maps (SOMs) are well known in environmetric studies (Tsakovski et al., 2009; Skwarzec et al., 2009; Simeonov et al., 2007) and have already been used for surface water quality analyses (Astel et al., 2007; Boszke and Astel, 2009), it is surprising that the technique has not been applied in the interpretation of spatiotemporal dynamics data for spring and stream water chemistry in a high-mountain area. Self-organizing maps of Kohonen, being resistant to departures from the rules concerning data distributions as well as to gaps in a data set, deliver extraordinary visualization ability coupled with classification tools (Astel et al., 2007; Zhang et al., 2008). Therefore, the purpose of the

* Corresponding author.
E-mail addresses: miroslaw.zelazny@uj.edu.pl (M. Żelazny), astel@apsl.edu.pl, AliAst@poczta.fm (A. Astel), rlmalek@cyf-kr.edu.pl (S. Małek).

0269-7491/$ – see front matter © 2010 Elsevier Ltd. All rights reserved.
doi:10.1016/j.envpol.2010.11.021

research was to explore natural spatiotemporal dynamics of spring and stream water chemical composition in the high mountain drainage basin of Chochołowski Stream. Additional aim was to characterize the usefulness of the SOM technique in the exploration and interpretation of hydrochemical data.

2. Materials and methods

2.1. Sampling site

The Tatras are the highest range in the Carpathian mountain belt and are located along the national border between Poland and Slovakia. The highest peak in the Carpathians, Mount Gerlach (2655 m a.s.l.), is located on the Slovak side. In Poland, the highest peak in the Tatras is Mount Rysy (2499 m a.s.l.). The drainage basin of Chochołowski Stream is located in the Western Tatras and receives water from the largest valley on the Polish side of the Tatra Mountains. The basin is also part of Tatrzański National Park (TNP), a biosphere reserve and a "Nature 2000" area. The Chochołowski Stream Basin has an area of 35 km^2 and is 11.1 km long. The mean rate of discharge in Chochołowski Stream is 1.27 $m^3 s^{-1}$ and specific discharge between 1983 and 1987 has been 36.4 $dm^3 s^{-1} km^{-2}$ (Krzemień, 1991). Fig. 1 shows the location of the Chochołowski Stream Basin.

The basin features a number of climate and vegetation zones. The mean annual air temperature ranges from 6 °C at lower elevations to nearly 4 °C at the highest elevations. At the higher elevations eight times more dynamic increase of an average annual temperature is observed. The calculated increase of average annual temperature at Kasprowy Wierch (1991 m a.s.l.) in the period between 1976 and 2000 is equal to 0.33 °C per 25 years while in Zakopane (857 m a.s.l) 0.04 °C per 25 years (Trepińska, 2004). In Hala Gąsienicowa the total annual precipitation in the period between 1927 and 2002 ranged from minimum 1.038 mm (1946) to 2.626 mm (2001), with an average value 1.689 mm and coefficient of variation equal to 17% (Niedźwiedź, 2003).

In the Western Matra Mts. (47% of the entire surface of the Tatra Mts.) a high percentage of grass-covered areas (44.1%) is to be noted, as well as lower than in the entire Tatras amount of rocky terrains (11.9%) (Guzik and Skawiński, 2009). The woodland vegetation zone begins at an elevation of 650 m a.s.l. and includes three kinds of forest. Lower forest extends between 650 and 1.250 m a.s.l., upper forest ranges from 1.250 to 1.550 m a.s.l. and dwarf mountain pine zone covers an area between 1.550 and 1.850 m a.s.l. (Guzik and Skawiński, 2009). The lower woodland belt consists of beech forest and in same ranges by beech-fir, fir – spruce or mainly artificial spruce stands. Beech stands (*Dentario glandulosae-Fagetum – Fagetum Carpaticum*) dominate across the earthen base course, abundant with calcium carbonate and a thin belt of spruce stands exists on poor moraines. Spruce forest stands (*Polysticho-Piceetum* and *Plagiothecio–Piceetum)* exist on limestone and granite rocks covering the upper woodland belt. Dwarf mountain pine covers nearly 37% of the area. The alpine (1.800–2.300 m a.s.l.) and subnival (2.300–2.499 m a.s.l.) belts occupy the highest elevations in the Tatra National Park (Guzik and Skawiński, 2009; Grodzińska et al., 2002).

The Chochołowski Stream Basin is very complex in terms of geology and tectonics. The southern part of the basin, a part of the main Tatra crystalline core, is formed of granitoid formations, gneiss, alaskite, mylonite, and crystalline shale. The basin consists of the High-Tatra zone and the sub-Tatra zone north of the crystalline core. The two zones are composed of sedimentary rocks – primarily limestone, dolomite, shale, marl with cherts, and sandstone (Bac-Moszaszwili et al., 1979; Krajewski, 2003). The waters of the Chochołowski Stream Basin and its component basins drain different types of rocks. Fig. 2 shows the geology of the Chochołowski Stream Basin, while Tables 1 and 2 show morphometric features of the sub-basins and percentages of various bedrock types in the Chochołowski Stream Basin, respectively.

The complex geologic and tectonic structure of the basin results in variability in water chemistry.

2.2. Spring and stream samples

The research was performed in the Chochołowski Stream Basin in the Western Tatra Mountains. A total of 31 unique sub-basins were identified along with 12 sampling sites found with increasing basin area along the main stream. Thirteen springs were also identified. Characteristics of the sub-basins and the location of the springs are shown in Table 3.

2.3. Analytical techniques

Measurements were performed once per month, starting in November of 2008 and ending in October of 2009. Physical and chemical data (pH, electrolytic conductivity (EC) [$\mu S\,cm^{-1}$]) were collected in the field using a WTW Multi350i meter with a POLYPLAST PRO-Hamilton (WTW, Germany) glass electrode and a WTW LR-325/01 conductometric sensor (WTW, Germany) with a built-in thermometer and a conductometric sensor constant of $k = 0.1$. The pH and EC of the water samples were double-checked once the samples had been delivered to the laboratory. In the winter, the samples were not analyzed until they had reached room temperature (about 20 °C). A 0.45 μm syringe filter was used to filter the water samples. The chemical composition of the water samples was determined using an ion chromatography system – DIONEX ICS 2000 (DIONEX, USA). A chromatographic system composed of two chromatographs – an anion module and a cation module – allows for the simultaneous separation and determination of 14 ions present in water: Ca^{2+}, Mg^{2+}, Na^+, K^+, HCO_3^-, SO_4^{2-}, Cl^-, NH_4^+, NO_3^-, NO_2^-, PO_4^{3-}, Li^+, Br^- and F^-. The aforesaid system was connected to an AS-40 autosampler and run using Chromeleon 6.70 software. The accuracy of the output was estimated based on certified

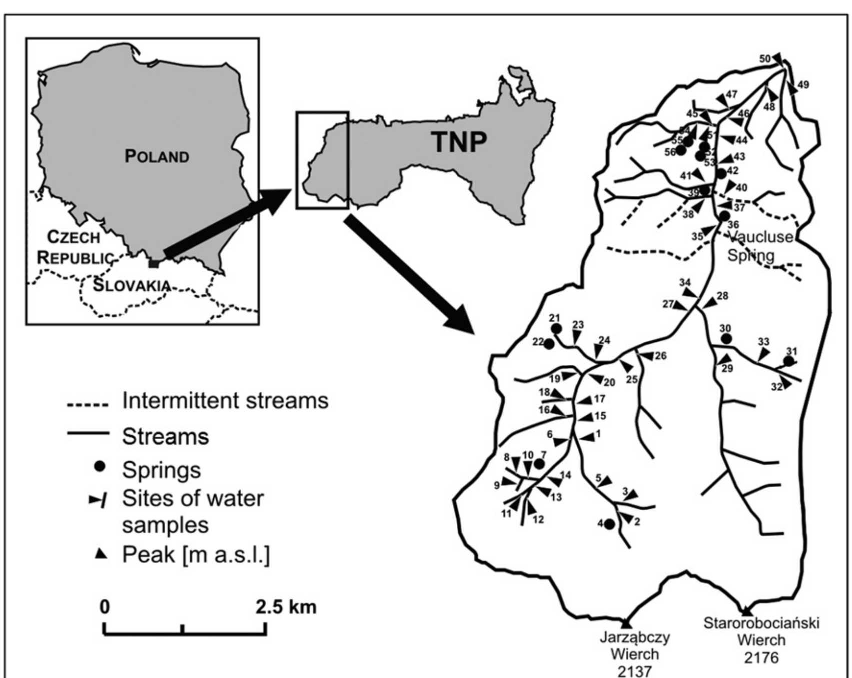

Fig. 1. Location of study area.

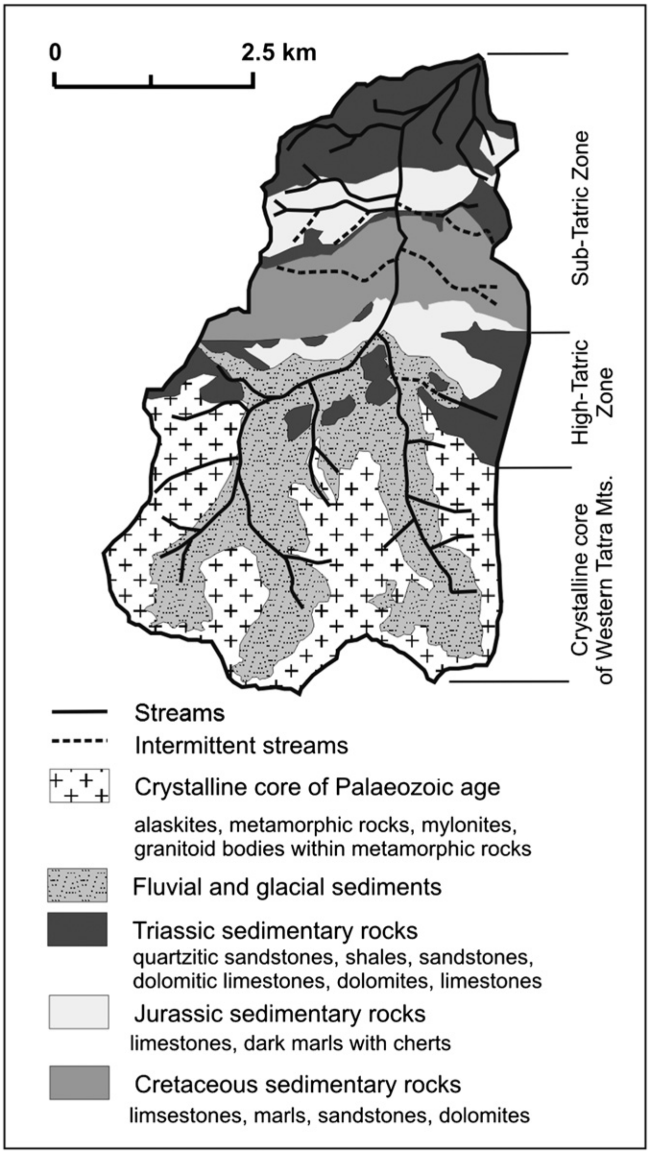

Fig. 2. Geologic structure of the Chochołowska Valley.

reference materials (AES-02, lot no. 901, a low pH acid rain sample, Trois-94, lot no. 306, colored soft water from Quebec), residue analysis, and comparative analysis using ICP-MS. The obtained results were consecutively evaluated statistically basing on samples which fulfill the criteria of ionic balance according to PN-C-04638-02 standard (PN, 1989). Dissolved organic carbon was not measured and included in ionic balance calculations since it is not taken into consideration in the PN-C-04638-02 standard. When the concentration of an analyte was below the detection limit, the code NaN (Not a Number) was inserted to the raw data set due to software requirements. Fortunately, the self-organizing map algorithm implemented in the Matlab environment as a SOM Toolbox has the ability to deal with the missing data. If an observation is missing a value on a specific variable, and hence coded as NaN, that variable is omitted from the distance calculation for that observation (Sarkisian, 2008). As a result NaNs are neither treated as zero nor as lack of sample. Replacement code was used for K^+ (0.19% of all water samples), NH_4^+ (26.18%), and for more than 50% of the results in the case of NO_2^-, PO_4^{3-}, Li^+, and Br^-. Due to a high number of replacements, NO_2^-, PO_4^{3-}, Li^+, and Br^- were excluded from SOM analysis. EC was also excluded as its value is positively correlated with ion abundance, while pH was recalculated for H^+ [mg dm^{-3}].

Table 1
Morphometric features of the Chochołowski Stream Basin.

Morphometric parameter	Value	
Maximum elevation	m a.s.l.	2176
Minimum elevation	m a.s.l.	912
Mean elevation	m	1399
Area	km^2	33.3
Slope	%	28.4
Length	km	11.62

Table 2
Bedrock type percentages in the Chochołowski Stream Basin.

Bedrock	Basin area [%]
Fluvial and glacial sediments	32.01
Alaskite	9.45
Metamorphic rocks	6.91
Granitoid bodies within metamorphic rocks	6.65
Mylonite	5.49
Quartzitic sandstones, shale	4.15
Sandstone, calcareous conglomerates, limestone	4.52
Dolomitic limestone, limestone, dolomite	10.47
Dolomite, nodular limestone	3.73
Limestone, marl with cherts	2.23
Dolomite	2.10

2.4. Intelligent data analysis procedure

Various statistical multivariate techniques are commonly used for environmental data modelling and assessment (Astel, 2010). This research involved the use of the self-organizing map (SOM) algorithm – one of the most efficient neural network architectures for solving problems in the fields of exploratory data analysis, clustering, and data visualization. The theoretical background for the SOM approach can be found elsewhere (Kohonen, 1984, 1995; Kohonen et al., 1996; Vesanto, 2000; Giraudel and Lek, 2001; Fort, 2006; Cottrell et al., 1998), and hence this paper presents only key advantages related to both exceptional visualization, dimension reduction, and exploration abilities.

Table 3
Characteristics of sub-basins and springs in the Chochołowski Stream Basin.

ID	Characteristics of sub-basins			ID	Characteristics of sub-basins and springs		
	Maximum	Minimum	Total area		Maximum	Minimum	Total area
	Elevation in meters		km^2		Elevation in meters		km^2
51	1246	970	0.035	1	2137	1200	3.780
54	1246	970	0.045	29	2176	1100	6.435
18	1500	1150	0.243	15	2137	1175	6.759
47	1161	950	0.270	17	2137	1140	7.443
48	1276	940	0.270	28	2176	1040	8.217
32	1829	1275	0.270	20	2137	1120	8.478
8	1670	1370	0.288	25	2137	1100	9.936
3	1846	1355	0.315	27	2137	1040	12.744
11	2064	1380	0.324	34	2176	1030	21.051
16	1632	1175	0.549	35	2176	1010	24.696
41	1491	1000	0.585	37	2176	995	25.236
23	1663	1240	0.630	43	2176	970	27.774
12	1958	1380	0.630	44	2176	960	28.494
33	1829	1235	0.702	46	2176	950	29.457
19	1653	1120	0.720	50	2176	930	33.290
40	1448	1000	0.729	4	Springs	1315	
9	1670	1370	0.729	7		1380	
45	1400	960	0.873	21		1270	
49	1271	935	0.900	22		1260	
38	1491	995	0.900	30		1100	
24	1663	1150	0.918	31		1285	
10	1670	1350	1.053	36		1000	
13	2064	1350	1.089	39		995	
26	1765	1080	1.098	42		1000	
14	2064	1340	2.205	52		980	
2	2137	1360	2.430	53		975	
6	2064	1200	2.790	55		980	
5	2137	1250	3.150	56		980	

Note: Identification numbers (ID) in Table 3 refer to the numbers shown in Fig. 1.

Table 4
Basic statistics of physiochemical data.

Feature	Unit	Mean	Median	Min.	Max.	S.D.	Variability factor
pH		7.70	7.68	6.43	8.60	0.43	5.61
EC	[$\mu S\,cm^{-1}$]	143.2	74.2	14.4	416.0	122.6	85.65
H^+	[$mg\,dm^{-3}$]	0.000034	0.000021	0.0000025	0.00037	0.000046	134.24
	[$mEq\,dm^{-3}$]	0.000034	0.000021	0.0000025	0.00037	0.000046	
Ca^{2+}	[$mg\,dm^{-3}$]	19.69	8.47	1.42	67.77	18.68	94.86
	[$mEq\,dm^{-3}$]	0.98	0.42	0.07	3.38	0.96	
Mg^{2+}	[$mg\,dm^{-3}$]	7.61	3.70	0.34	30.38	7.85	103.11
	[$mEq\,dm^{-3}$]	0.63	0.30	0.03	2.50	0.65	
Na^+	[$mg\,dm^{-3}$]	0.80	0.84	0.14	2.08	0.32	39.90
	[$mEq\,dm^{-3}$]	0.035	0.037	0.006	0.090	0.014	
K^+	[$mg\,dm^{-3}$]	0.41	0.33	0.06	1.51	0.25	61.61
	[$mEq\,dm^{-3}$]	0.0105	0.0084	0.0015	0.0386	0.0064	
NH_4^+	[$mg\,dm^{-3}$]	0.023	0.007	0.002	0.68	0.043	191.08
	[$mEq\,dm^{-3}$]	0.00128	0.00039	0.00011	0.03770	0.00238	
HCO_3^-	[$mg\,dm^{-3}$]	90.01	40.68	1.56	309.4	89.03	98.92
	[$mEq\,dm^{-3}$]	1.48	0.67	0.03	5.07	1.46	
SO_4^{2-}	[$mg\,dm^{-3}$]	7.92	5.94	2.07	67.5	6.39	80.65
	[$mEq\,dm^{-3}$]	0.16	0.12	0.04	1.41	0.13	
Cl^-	[$mg\,dm^{-3}$]	0.48	0.35	0.08	2.60	0.33	69.40
	[$mEq\,dm^{-3}$]	0.0135	0.0099	0.0023	0.0733	0.0093	
NO_3^-	[$mg\,dm^{-3}$]	1.64	1.45	0.03	4.81	0.88	53.69
	[$mEq\,dm^{-3}$]	0.0264	0.0234	0.0005	0.0776	0.0142	
F^-	[$mg\,dm^{-3}$]	0.029	0.026	0.0003	0.12	0.015	53.14
	[$mEq\,dm^{-3}$]	0.001526	0.001369	0.000016	0.006316	0.000790	

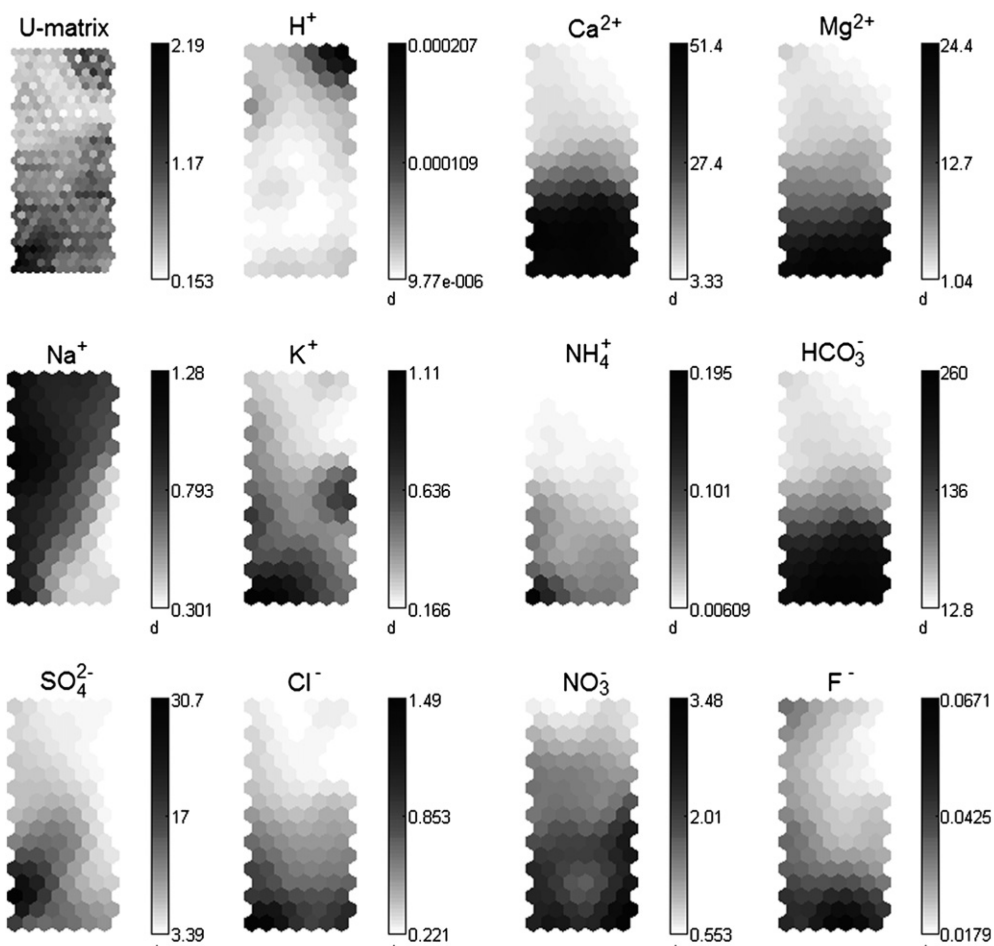

Fig. 3. SOM planes for entire set of variables and all spring and stream water samples.

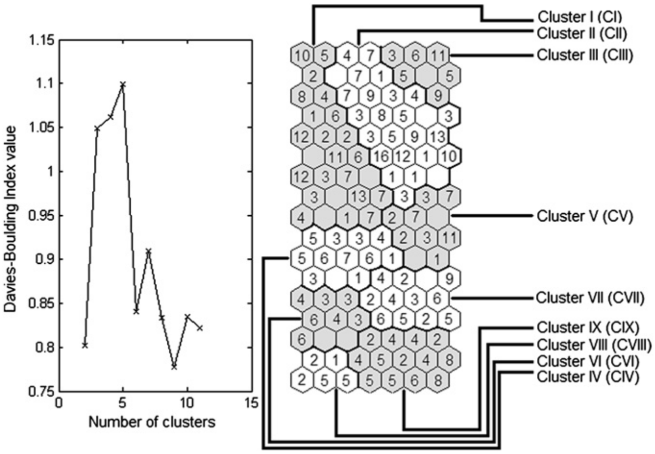

Fig. 4. Clustering pattern according to the Davies–Bouldin index minimum value.

2.4.1. General idea

The SOM algorithm, much like conventional ordination methods, shares the basic idea of displaying a high-dimensional signal manifold onto a much lower dimensional network in an orderly fashion (usually 2D space). The SOM produces virtual communities in a low dimensional lattice through an unsupervised learning process. The term "self-organizing" refers to the ability to learn and organize information without being given the associated-dependent output values for the input pattern (Mukherjee, 1997). The SOM is noise tolerant; this property is highly desirable when site-measured data are used. The advantages of the SOM in relation to conventional ordination methods as principal component analysis and cluster analysis are discussed elsewhere (Astel et al., 2007; Zhang et al., 2008).

2.4.2. Kohonen's neural network map description

The SOM consists of neurons organized on a regular, usually two-dimensional grid. The neurons are connected to adjacent neurons by a neighborhood relation, which dictates the topology, or structure of the map and thus similar water samples should be mapped close together on a grid. In time-iterative training, an algorithm constructs grid-nodes in the SOM in order to represent the whole data set, and their weights are optimized. Thus, an optimal topology is expected. When the SOM net has been trained, the map needs to be evaluated to find out if it has been optimally trained, or if further training is required. The number of grid nodes to be used in the SOM analysis may vary from a few dozen up to several thousand, and can be considered as a trade-off between representation accuracy. A small number of grid nodes will result in a high quantization error (QE, scaled as 1-0) and well-defined clusters, while a large number of grid nodes results in a low quantization error and, in the most extreme case, a cluster for each data sample. In other words the lower quantization error the higher number of clusters to be interpreted. In order to assess the SOM topology, preservation is quantified and represented by a topographic error (TE) (Kohonen, 2001). The lower the topographic error (close to 0), the better the SOM preserves the topology (Arsuaga and Díaz, 2006). Unfortunately, there are no reference values of QE and TE. They strongly depend on the map resolution. According to Peeters et al. (2006), quantization error rapidly decreases with increasing number of grid nodes, while topographic error converges to a stable value. As suggested by Vesanto et al. (2000), the most satisfactory compromise between clustering ability, quantization error, and topographic error could be achieved when the number of nodes (n) is determined using the following formula: $n = 5\sqrt{\text{number of samples}}$.

2.4.3. Similarities and classification

When several features are considered, it is difficult to compare all maps for all features and in order to accomplish water samples' classification, it becomes

Table 5
Statistical analysis (Kruskal–Wallis Test and Dunn Test) of differences between H^+, Ca^{2+}, Mg^{2+}, Na^+, K^+, NH_4^+, HCO_3^-, SO_4^{2-}, Cl^-, NO_3^-, and F^- median values in the combination of clusters obtained using the SOM approach (* − $p < 0.05$; ** − $p < 0.01$, *** − $p < 0.001$).

Feature	H^+	Ca^{2+}	Mg^{2+}	Na^+	K^+	NH_4^+	HCO_3^-	SO_4^{2-}	Cl^-	NO_3^-	F^-
Kruskal–Wallis Test ($p < 0.001$)	230	440	430	360	340	240	430	350	410	280	280
Dunn's Test (* − $p < 0.05$; ** − $p < 0.01$; *** − $p < 0.001$, n.s. − not significant)											
CI vs CII	*	***	n.s.	***	***	n.s.	n.s.	***	***	*	***
CI vs CIII	***	***	***	***	***	n.s.	***	***	n.s.	***	***
CI vs CIV	**	***	***	***	**	***	***	**	***	***	n.s.
CI vs CV	n.s.	n.s.	n.s.	***	***	n.s.	n.s.	***	*	**	n.s.
CI vs CVI	**	***	***	*	**	***	***	***	***	***	***
CI vs CVII	***	***	***	***	n.s.	***	***	n.s.	***	***	n.s.
CI vs CVIII	n.s.	***	***	n.s.	***	***	***	n.s.	***	***	n.s.
CI vs CIX	*	***	***	***	***	***	***	**	***	***	***
CII vs CIII	***	n.s.	*	n.s.	n.s.	n.s.	n.s.	n.s.	n.s.	n.s.	n.s.
CII vs CIV	***	***	***	n.s.	***	***	***	***	***	***	***
CII vs CV	n.s.	***	***	***	***	n.s.	***	n.s.	***	***	*
CII vs CVI	***	***	***	n.s.	***	***	***	***	***	***	***
CII vs CVII	***	***	***	***	***	***	***	***	***	***	***
CII vs CVIII	n.s.	***	***	n.s.	***	***	***	***	***	***	***
CII vs CIX	***	***	***	***	***	***	***	***	***	***	***
CIII vs CIV	***	***	***	n.s.	***	***	***	***	***	***	***
CIII vs CV	***	***	***	***	***	n.s.	***	n.s.	***	***	n.s.
CIII vs CVI	***	***	***	n.s.	***	***	***	***	***	***	***
CIII vs CVII	***	***	***	***	***	***	***	***	***	***	***
CIII vs CVIII	***	***	***	n.s.	***	***	***	***	***	***	***
CIII vs CIX	***	***	***	***	***	***	***	***	***	***	***
CIV vs CV	n.s.	n.s.	n.s.	***	n.s.	***	n.s.	***	n.s.	n.s.	n.s.
CIV vs CVI	n.s.	*	n.s.	n.s.	n.s.	n.s.	n.s.	n.s.	n.s.	n.s.	*
CIV vs CVII	n.s.	n.s.	n.s.	***	n.s.	n.s.	n.s.	***	n.s.	n.s.	n.s.
CIV vs CVIII	n.s.	n.s.	n.s.	n.s.	*	n.s.	n.s.	n.s.	n.s.	n.s.	n.s.
CIV vs CIX	n.s.	*	***	***	n.s.	n.s.	***	n.s.	n.s.	n.s.	***
CV vs CVI	n.s.	***	**	***	n.s.	***	**	***	n.s.	n.s.	***
CV vs CVII	***	***	**	n.s.	**	***	***	***	n.s.	n.s.	n.s.
CV vs CVIII	n.s.	*	***	***	n.s.	***	**	***	**	n.s.	n.s.
CV vs CIX	n.s.	***	***	n.s.	n.s.	***	***	***	***	n.s.	***
CVI vs CVII	n.s.	n.s.	n.s.	***	n.s.	n.s.	n.s.	***	n.s.	n.s.	n.s.
CVI vs CVIII	n.s.	n.s.	n.s.	n.s.	n.s.	n.s.	n.s.	n.s.	n.s.	n.s.	n.s.
CVI vs CIX	n.s.	n.s.	n.s.	***	n.s.	n.s.	n.s.	n.s.	n.s.	n.s.	n.s.
CVII vs CVIII	n.s.	n.s.	n.s.	***	***	n.s.	n.s.	n.s.	n.s.	n.s.	n.s.
CVII vs CIX	n.s.	n.s.	n.s.	n.s.	*	n.s.	n.s.	**	n.s.	n.s.	***
CVIII vs CIX	n.s.	n.s.	n.s.	***	n.s.	n.s.	n.s.	n.s.	n.s.	n.s.	n.s.

necessary to find similarity in the features', and simultaneously, in the samples' space. Input features planes (e.g. variables) could be visualized on a summary SOM map (also called a unified distance matrix; U-matrix) to show the contribution of each feature in the self-organization of the map (Park et al., 2003). The U-matrix visualizes distances between neighboring map units, and helps to identify cluster structure of the map: high values of the U-matrix indicate a cluster border, uniform areas of low values indicate clusters themselves (Ultsch and Siemon, 1990), while each feature plane shows the values of a feature of weight vectors (which correspond to a certain variable). Feature planes can be considered as a sliced version of the SOM map and provide a powerful tool to analyze the community structure. In other words, a U-matrix expresses semi-quantitative information about the distribution of a complete set of variables for a complete set of objects while a separate feature plane visualizes the distribution of a particular feature for a complete set of objects. Because of this, a U-matrix joined with features planes can be effectively applied in the assessment of inter-feature and inter-object relations.

The non-hierarchical K-means algorithm was applied in a clustering step. Different numbers of predefined clusters were tried, and finally, the best classification with the lowest Davies–Bouldin (DB) index (a function of the ratio of the sum of within-cluster scatter and between-cluster separation) (Davies and Bouldin, 1979) was chosen. In order to assess the significance of the clustering pattern, non-parametric tests such as the Kruskal–Wallis's and the Dunn's Tests were used. All calculations in this study were performed using Matlab 2007 (MathWorks, Inc.), Prism 5 Trial Version (GraphPad Software, Inc.), Statistica 9.0 (Statsoft, Inc.,) and AquaChem v 5.0 software running on a Windows VISTA platform.

3. Results

Table 4 shows pH, EC, and other chemical data for the spring and stream water samples collected in the Chochołowski Stream Basin. The chemical composition of water is characterized by a relatively high concentration of bicarbonate and calcium ions. Other key ions include sulfate, magnesium, and sometimes sodium. Low concentrations of biogenic compounds such as NO_3^- and NH_4^+ were detected, while NO_2^- and PO_4^{3-} were not found to be present. This indicates little eutrophication of the water. F^- concentrations were also determined to be low, while Li^+ and Br^- were not detected at all. The area's very complex geologic structure is reflected in the wide range of ion concentrations detected. This is also confirmed by the value of the variability factor, which is especially high in the case of common ions such as HCO_3^-, Mg^{2+}, and NH_4^+.

Prior to the analysis of spatiotemporal dynamics of spring and stream water chemical composition in the Chochołowski Stream Basin, a total of 5,841 analytical results were arranged in a two-way array of constant dimensions of 11 variables (H^+, Ca^{2+}, Mg^{2+}, Na^+, K^+, NH_4^+, HCO_3^-, SO_4^{2-}, Cl^-, NO_3^-, F^-) and 531 water samples collected at 56 sampling locations. The dimensionality of Kohonen's map was determined as 10×21 grid nodes ($n = 5\sqrt{531} = 115.2$) based on the formula shown earlier. In light of a number of possible combinations of final dimensions (i.e. 15×8, 14×8, and 17×7 grid nodes) QE and TE were calculated in all cases. For 15×8 and 14×8, QE and TE were equal to 1.096, 1.093, and 0.058, 0.049, respectively, while for 17×7, the selected "proper" dimension, QE and TE were equal to 1.085 and 0.034. Moreover, a hexagonal lattice was preferred because it does not favor either the horizontal or vertical direction (Kohonen, 2001). Once the SOM's grid had been optimized, the U-matrix and individual features planes were visualized. The nonlinear projection of chemical features' abundance variability for all sampling sites in the Chochołowski Stream Basin together with the U-matrix plane are presented in Fig. 3.

A visual assessment of the U-matrix and features planes (Fig. 3) enabled an assessment of similarities both in the objects' (water samples) as well as features' space. In general, the lower area of the U-matrix plane represented water samples with a relatively high abundance of most ions (Ca^{2+}, Mg^{2+}, HCO_3^-, NO_3^-, F^-), while upper right area samples possessed a high concentration of H^+. The highly differentiated grey scale of the U-matrix and the feature planes suggested the existence of several similarity groups in the set of water samples based on their location and/or temporal variation. Thus, the spring and stream water samples were clustered based on the K-means clustering mode. Different values of k (predefined number of clusters) were tested and the sum of squares for each run was calculated. The best classification (nine-cluster configuration) with the lowest DB index (a function of the ratio of the sum of within-cluster scatter and between-cluster separation) was chosen (Fig. 4). Setting up Figs. 3 and 4 allowed association of a clustering pattern with features' abundance variability according to clusters border. In other words, the overall chemical composition of water samples included to the specific cluster could be assessed by analysis of the grey scale pattern of corresponding fragment of the feature planes. The differences between median values of concentration of ions in the combination of clusters obtained using the SOM were statistically evaluated and results are depicted in Table 5).

Clusters I-IX (consecutively named CI-CIX) included various numbers of the 531 water samples available, according to seasonal variability as follows: CI – 126 (spring (s) – 34, summer (su) – 25, autumn (a) – 13, winter (w) – 54), CII – 135 (s – 47, su – 56, a – 8, w – 24), CIII – 39 (s – 14, su – 14, a – 4, w – 7), CIV – 44 (s – 7, su – 23, a – 8, w – 6), CV – 36 (s – 8, su – 16, a – 3, w – 9), CVI – 29 (s – 10, su – 10, a – 2, w – 7), CVII – 48 (s – 18, su – 21, a – 2, w – 7), CVIII – 15 (s – 2, su – 1, a – 3, w – 9) and CIX – 59 (s – 14, su – 18, a – 7, w – 20). Water samples assigned to each cluster were identified

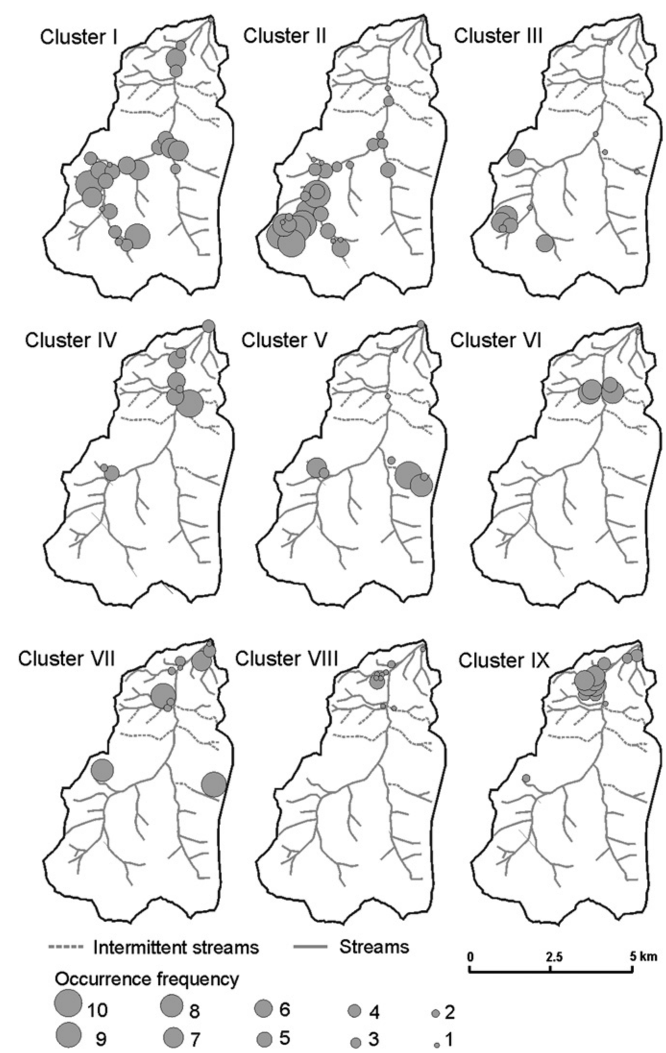

Fig. 5. Visualization of the clusters composition according to geographical location of the sampling points.

and plotted on a geographic map in order to show spatial patterns (Fig. 5). The occurrence frequency was presented in the form of circles of various diameter. The higher circle diameter the higher number of water samples collected in a specific location assigned to a given cluster. Such visualization enabled discovering spatial range of clusters in order to associate chemical composition of spring and stream water samples with seasonality as well as land and rock characteristics.

A comparison of initially determined values of physical and chemical parameters with the classification results allowed for the assignment of clustering patterns to factors impacting the quality of water (Figs. 6 and 7).

Moreover, it was of substantial importance to comment on the content of each cluster of spring and stream water samples in order to better understand the relationships between the physical and chemical parameters measured and the samples' locations. Waters draining the main part of the Chochołowski Stream Basin were grouped into two of the largest clusters (CI and CII). The first cluster includes water samples collected mostly in the winter (43%) and spring (27%). These samples are characterized by a pH of 7.6, low average mineralization (55.68 mg dm^{-3}) (Fig. 7), and low concentrations of most ions, with the exception of Na^+ (Fig. 6). The spring and stream waters included in CI cover about 95% of the total area of the drainage basin – excluding the Upper Chochołowski Stream Basin (Fig. 5). The chemical composition of samples collected in Chochołowski Stream and its sub-basins is quite similar during dry periods in the winter and spring. There is a marked decrease in the amount of water leaving the Tatra Mountains in the wintertime. Surface runoff is negligible during long cold winters. Water freezes in small side streams and runoff ceases to take place. The winter season is characterized by substantial groundwater runoff, especially in the High Tatras, given how rarely midwinter snowmelt takes place (Łajczak, 1988). In the upper part of the basin, water circulates within large fluvioglacial formations, which extends its contact time with the parent rock material. Based on contemporary morphometric data provided by Klapyda, the walls of terminal moraines are 25–30 m thick, while their thickness inside the ablation moraine cirque is 15–20 m. This is associated with higher mineralization of water, especially increased sodium ion content, which is released by weathering processes affecting glacial sediments (Małecka, 1989; Mizerski and Sylwestrzak, 2002; Kostrakiewicz, 1996). The highest concentration of dissolved salts was also identified by Krzemień (1982, 1990) in Starobociański Stream. The reason for such high concentrations was related to the drainage of the crystalline core in the winter.

Water samples included in CII were collected mostly in the spring (35%) and summer (41.5%) from the Upper Chochołowski Stream sub-basin, which drains the highest part of the Chochołowski Stream Basin and the main stretch of Chochołowski Stream (Fig. 5). This section of the stream is located in the crystalline part of the basin and begins at the main Chochołowski Vauclause Spring. CII consisted of spring and stream water samples characterized by ion concentrations that were lower than those in CI (Fig. 6). The sodium ion concentration was high, as was the case in CI; the pH was 7.47, and average mineralization was significantly lower (38.9 mg dm^{-3}) (Fig. 7). CII reflects water chemistry in the

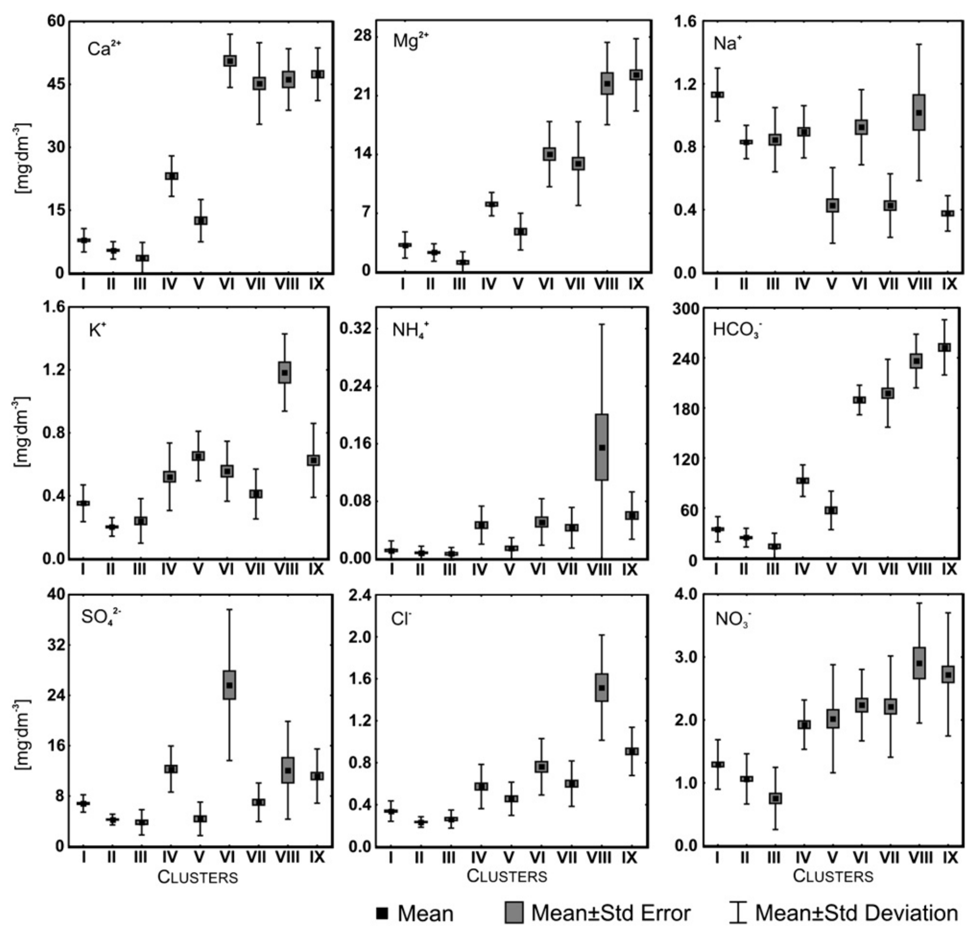

Fig. 6. Ion concentrations according to clustering pattern.

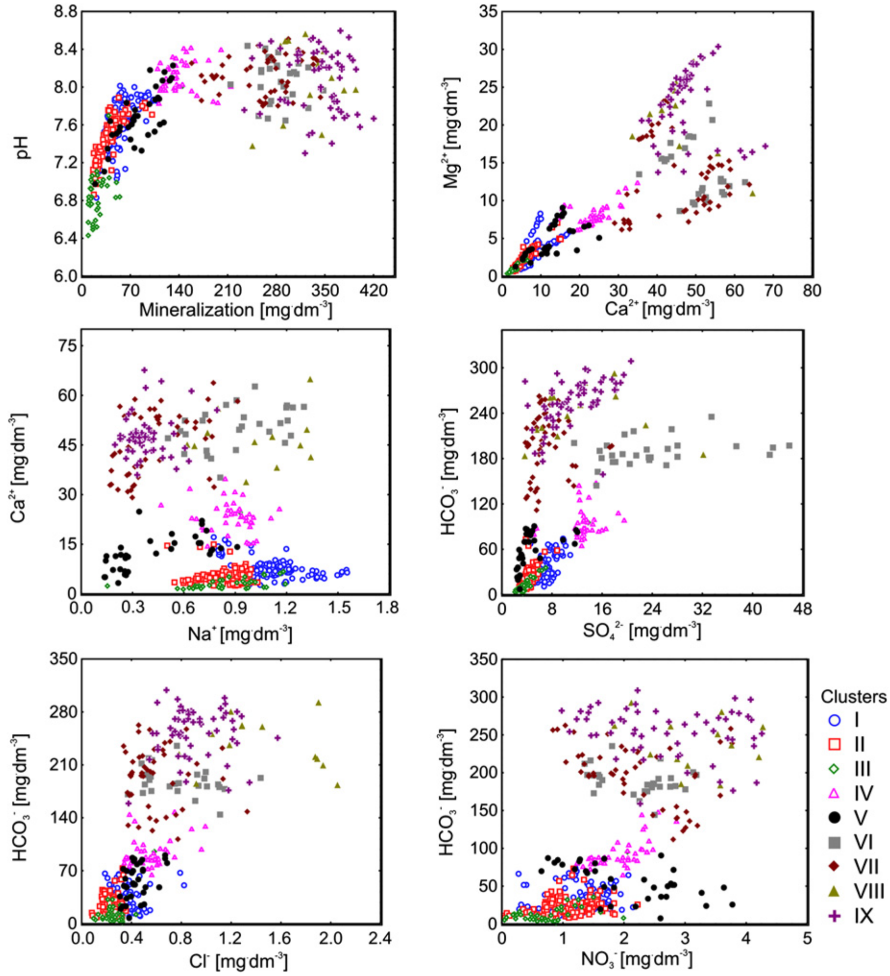

Fig. 7. Relationship between different ions and clusters.

Chochołowski Stream Basin at the time of spring snowmelt and summer elevated water levels.

The springs and small streams found at the highest elevations in the Chochołowski Stream Basin were grouped in CIII (Fig. 5). The water chemistry of this group is characterized by the lowest ion concentrations in all the clusters identified (Fig. 6), a slightly acidic pH (6.88), and mineralization of 24.81 mg dm^{-3} (Fig. 7). The water chemistry in this cluster is generally uniform in the spring and summer. Low water ion concentrations in the crystalline part of the basin are the result of fast water circulation, which leads to little contact with the parent rock material (Małecka, 1989). An acidic pH might be produced by mountain pine as well as blueberry plants as a result of acidic organic litterfall. The high Na^+ content in CI-CIII is the result of the leaching of rocks forming the crystalline core. The rocks are made primarily of quartz, feldspar, and mica, which are rich in sodium aluminosilicate, potassium, calcium, and magnesium (Kostrakiewicz, 1996; Oleksynowa and Komornicki, 1996).

The influence of Chochołowski Spring on the entire stream's water chemistry is particularly interesting and appears starting with the samples included in CIV. The Chochołowski Vaucluse Spring is a karst-type spring with a very high rate of discharge (400–600 dm^3 s^{-1}) (Barczyk et al., 2000; Małecka, 1993, 1997). The spring is recharged with water flowing through a system of fissures created in a fault zone from Szczelina Chochołowska Cave and Rybia Cave. Other sources of supply include the Kominiarski Wierch Massif, and to some extent, Chochołowski Stream itself. The area recharging Chochołowski Spring consists of carbonate formations of the High-Tatra zone, which are known to have a large water retention capacity (Barczyk, 2004, 2008; Rogalski, 1984).

The water chemistry of Chochołowski Stream is determined by its spring's water chemistry, starting from the spring itself and ending at the edge of its drainage basin, despite the fact that the basin highly loaded with ionic substances from adjacent basins. Chochołowski Stream is recharged largely by groundwater and its large spring area (Łajczak, 1988). The chemical composition of the spring and the stream is characterized by significantly higher mineralization (140 mg dm^{-3}), and hence higher concentrations of particular ions than those in other clusters (Figs. 6 and 7). The spring's influence on water chemistry is particularly apparent during the autumn dry period when deep circulation water plays a very important role during the winter as well as other drier periods (Łajczak, 1988).

CV represents the chemistry of streams draining mixed-type basins featuring crystalline and sedimentary rocks. The average water pH is 7.67 and mineralization is 82.5 mg dm^{-3} (Fig. 7). Mixed-type basins are characterized by large fluctuations in pH (6.98–8.23) and mineralization (18.74–130.52 mg dm^{-3}). The concentration of most ions, except K^+, is low (Fig. 6). CV explains the high K^+ concentration, which is the result of crystalline rock weathering. Other explanations for the K^+ include leaching from spruce canopies (Małek and Astel, 2008) and elevated weathering rates (Małek et al., 2005), especially evident in the summer. CV possesses characteristics of both crystalline and sedimentary origin.

CVI includes very deep circulation waters, which drain a part of the basin with a very complex geologic structure including tectonic faults. The parent material in this part of the Chochołowski Stream Basin includes shale and marl, which may block crevices in the fault zone and cause deep circulation groundwater to reach the surface (Barczyk, 2008). This type of groundwater is characterized by high average mineralization (284.3 mg dm^{-3}), high ion concentrations, and high pH (8.06) (Figs. 6 and 7). Waters included in CVI are distinguished by very high SO_4^{2-} concentrations (25.6 mg dm^{-3}). Given that most samples were collected in the spring and early summer, CVI reflects a specific temporal variation, where the chemical composition of samples is affected by significant groundwater influx driven by the melting of snow, which is the principal source of groundwater recharge in the basin (Łajczak, 1988, 1996).

Waters draining small karst-type and mixed-type basins included in CVII are characterized by a pH of 8.14, very high average mineralization (266 mg dm^{-3}) (Fig. 7), as well as high ion concentrations, except for Na^+ and SO_4^{2-} (Fig. 6). It should be emphasized that the majority of samples included in CVII were collected in the spring and summer. Periods of late spring snowmelt and summer precipitation lead to peak runoff rates, which leads to peak ion outflow from the basin (Łajczak, 1988).

The last two clusters (VIII and IX) included water samples collected in basins featuring carbonate parent material, which is relatively easily leached. Geographically, they cover the northern part (lowest elevation) of the Chochołowski Stream Basin, where water circulates within a slope of average gradient – entirely covered by spruce forest – and features very high mineralization (323.58 mg dm^{-3} and 339.31 mg dm^{-3}, respectively for cluster VIII and IX) (Fig. 7), high ion concentrations (except Na^+), and high concentrations of biogenic ions, especially NH_4^+ (Fig. 6). The CVIII and CIX chemical composition reflects a specific time period, as the majority of water samples were collected in the winter at low water levels. Low wintertime temperatures favor decreased surface runoff and increased significance of groundwater recharge. This results in higher mineralization in the water (Łajczak, 1988; Kostrakiewicz, 1996; Żelazny et al., 2007).

4. Conclusions

The method used in this research allowed for a logical spatio-temporal grouping of chemical composition data for waters collected from high mountain areas with a complex geologic structure. The chemical composition map produced consists of nine clusters and shows not only the effects of geologic structure but also of hydro-geochemical relationships in surface waters and spring waters. These relationships are based on snowmelt effects, floods, winter dry periods, and summer dry periods. The southern crystalline part of the basin is characterized by low mineralization (<60 mg/l) and low ion concentrations (except Na^+ and H^+). The low pH, detected primarily in springs during the spring season and the summer season, is the result of deep circulation in virtually insoluble crystalline core rocks such as quartz, feldspar, and mica, which are rich in sodium aluminosilicate, potassium, calcium, and magnesium. The northern part of the Chochołowska Valley – formed of sedimentary rocks, primarily limestone, dolomite, shale, marl with cherts, and sandstone – is characterized by significantly higher ion concentrations, and hence mineralization. This is especially true of lateral sub-basins. The chemistry of the downstream stretch of Chochołowski Stream depends on the Wywierzysko Chochołowskie Spring. The Spring's rate of discharge is large enough that it determines the Stream's water chemistry as far as the edge of the Tatra Mountains. Finally, eutrophication has not been shown to be a threat in the Chochołowska Valley. Obtained results and their interpretation proved that self-organizing maps can be used to unravel spatial and temporal patterns and dynamics in hydrochemically and hydrologically complex catchments.

Acknowledgments

Tatra National Park – for making digital maps and the DEM available. Piotr Kłapyda, Project No. MNiSW NN306282235. Late Glacial and Holocene Stages of High Mountain Relief Evolution – Western Tatra Mountain Case Study.

The research is a part of the following project: *"Factors determining spatial variability and dynamics of water chemical composition in Tatra National Park"*, financed by the Polish Ministry of Science and Higher Education (MNiSW–N305 081 32/2824) – Project Director: M. Żelazny; as well as was financially supported within the framework of project BW/7/9009028/10 given by Pomeranian Academy.

References

Allan, J.D., Flecker, A.S., 1993. Biodiversity conservation in running waters. BioScience 43, 32–43.
Arsuaga, U.A., Díaz, M.F., 2006. Topology preservation in SOM. Proceedings of World Academy of Science, Engineering and Technology 16, 187–190.
Astel, A., Astel, K., Biziuk, M., Namieśnik, J., 2006. Classification of drinking water samples using the Chernoff's Faces visualization approach. Polish Journal of Environmental Studies 15 (5), 691–697.
Astel, A., Tsakovski, S., Barbieri, P., Simeonov, V., 2007. Comparison of self-organizing maps classification approach with cluster and principal components analysis for large environmental data sets. Water Research 41, 4566–4578.
Astel, A., Małek, S., Krakowian, K., 2009. Multivariate exploration and classification applied to the chemical composition of spring waters in sanctuary forest areas. International Journal of Environmental Analytical Chemistry 89 (8–12), 597–620.
Astel, A., 2010. Multivariate statistical modelling of water and soil related environmental compartments. In: Hanrahan, G. (Ed.), Modelling of Pollutants in Complex Environmental Systems, vol. II. ILM Publications, pp. 151–212.
Bac-Moszaszwili, M., Burchart, J., Głazek, J., Iwanow, A., Jaroszewski, W., Kotański, Z., Lefeld, J., Mastella, L., Ziomkowski, W., Roniewicz, P., Skupiński, A., Westwalewicz-Mogilska, E., 1979. Geological map of the Polish Tatra Mts. 1:30 000 scale. Institute of Geology, Warsaw, Poland.
Barczyk, G., Jach, R., Nowicki, T., 2000. Chochołowska Valley Karst. In: Materials of 34 Speological Symposium, Cracow, pp. 9–20 (in polish).
Barczyk, G., 2004. Recent results of dye tracer tests of the Chochołowskie Vaucluse Spring Karst System (Western Tatra Mts.). Acta Geologica Polonica 54, 169–177.
Barczyk, G., 2008. Tatrzańskie wywierzyska: krasowe systemy wywierzyskowe Tatr Polskich. Tatrzański Park Narodowy, Zakopane, Poland, pp. 178 (in polish).
Boszke, L., Astel, A., 2009. Application of neural network-based modeling in assessment of mercury pollution level in the middle part of the Warta River. Environmental Monitoring Assessment 152 (1–4), 133–147.
Cottrell, M., Fort, J.C., Pagès, G., 1998. Theoretical aspects of the SOM algorithm. Neurocomputing 21, 119–138.
Davies, D.L., Bouldin, D.W., 1979. A cluster separation measure. Proceedings of the IEEE Transactions on Pattern Recognition and Machine Intelligence 1 (2), 224–227.
Fort, J.C., 2006. SOM's mathematics. Neural Networks 19, 812–816.
Giraudel, J.L., Lek, S., 2001. A comparison of self-organizing map algorithm and some conventional statistical methods for ecological community ordination. Ecological Modelling 146, 329–339.
Grodzińska, K., Godzik, B., Badea, O., Barancok, P., Istona, J., Matejka, K., Moravčik, P., Niemtur, S., Oszlányi, J., Parpan, V., Varsavová, M., Bytnerowicz, A., Szaro, R., 2002. Vegetation of selected forest stands in the Carpathian Mountains. In: Szaro, R.C., Bytnerowicz, A., Oszlányi, J. (Eds.), Effects of Air Pollution on Forest Health and Biodiversity in Forests of the Carpathian Mountains. Nato Science Series. IOS Press, Amsterdam, The Netherlands, pp. 96–117.
Guzik, M., Skawiński, P., 2009. Applying geomathics to determination of landscape altitudinal zones in the mountains. Landform Analysis 11, 25–32.
Kohonen, T., 1984. Self-organization and Associative Memory. Springer Verlag, Berlin, Germany.
Kohonen, T., 1995. Self-organizing Maps. Springer Inc., New York, USA.
Kohonen, T., 2001. Self-organizing Maps, third ed. Springer, Berlin, Germany.
Kohonen, T., Oja, E., Simula, O., Visa, A., Kangas, J., 1996. Engineering applications of the self-organizing map. Proceeding of the IEEE 84, 1358–1384.
Kopáček, J., Kaňa, J., Šantrůčková, H., Picek, T., Stuchlík, E., 2004. Chemical and biochemical characteristics of alpine soils in the Tatra Mountains and their correlation with lake water quality. Water, Air, and Soil Pollution 153 (1–4), 307–327.
Kostrakiewicz, L., 1996. Regionalizacja hydrochemiczna źródeł polskich Karpat Wewnętrznych. Wszechświat 9, 196–199 (in polish).

Krajewski, P.K., 2003. Facies development and lithostratigraphy of the Higtatric mid-Cretaceous (Zabijak Formation) in the Polish Tatra Mountains. Studia Geologica Polonica 121, 81–158.
Křeček, J., Turek, J., Ljungren, E., Stuchlík, E., Šporka, F., 2006. Hydrological processes in small catchments of mountain headwater lakes: the Tatra Mountains. Biologia Section Zoology, Bratislava 61 (Suppl. 18), 1–10.
Krzemień, K., 1982. Removal of dissolved material from the Starorobociański Stream crystalline catchment basin (The Western Tatra Mts). Studia Geomorphologica Carpatho-Balcanica 15, 71–80.
Krzemień, K., 1990. Związek przewodności właściwej wody i koncentracji materiału rozpuszczonego w obszarach o różnej budowie geologicznej. Zeszyty Naukowe UJ, Prace Geograficzne 77, 81–91 (in polish).
Krzemień, K., 1991. Dynamika wysokogórskiego systemu fluwialnego na przykładzie Tatr Zachodnich. Rozprawy Habilitacyjne Uniwersytet Jagielloński 215, 160 (in polish).
Łajczak, A., 1988. Opady i odpływ w polskich Tatrach w świetle pomiarów wieloletnich. Czasopismo Geograficzne 2, 137–170 (in polish).
Łajczak, A., 1996. Hydrologia. In: Mirek, Z. (Ed.), Przyroda Tatrzańskiego Parku Narodowego. Tatrzański Park Narodowy, Kraków-Zakopane, pp. 167–196 (in polish).
Małecka, D., 1989. Wpływ opadów atmosferycznych na kształtowanie chemizmu wód w obrębie masywu tatrzańskiego. Przegląd Geologiczny 10, 504–510 (in polish).
Małecka, D., 1993. Hydrogeologia Krasu Tatrzańskiego. In: Grodziński, J. (Ed.), Jaskinie Tatrzańskiego Parku Narodowego, vol. 3, pp. 11–35 (in polish).
Małecka, D., 1997. Źródła masywu tatrzańskiego. Acta Universitatis Lodzienss Folia Geographica Physica 2, 2–25 (in polish).
Małek, S., Astel, A., 2008. Throughfall chemistry in a spruce chronosequence in southern Poland. Environmental Pollution 155 (3), 517–527.
Małek, S., Martinson, L., Sverdrup, H., 2005. Modelling future soil chemistry at a highly polluted forest site at Istebna in Southern Poland using the "SAFE" model. Environmental Pollution 137 (3), 568–573.
Mizerski, W., Sylwestrzak, H., 2002. Słownik geologiczny. PWN, Warszawa, Poland, pp. 242 (in polish).
Mukherjee, A., 1997. Self-organizing neural network for identification of natural modes. Journal of Computing in Civil Engineering 11 (1), 74–77.
Niedźwiedź, T., 2003. Extreme precipitation events on the northern side of the Tatra Mountains. Geographica Polonica 76 (2), 15–23.
Oleksynowa, K., Komornicki, T., 1960. Materiały do znajomości wód w Tatrach Cz. V. Dolina Chochołowska. In: olnictwo, 7. Zeszyty Naukowe WSR w Krakowie, R. 117–148.
Oleksynowa, K., 1970. Charakterystyka geochemiczna wód tatrzańskich. Acta Hydrobiologica 12 (1), 1–110 (in polish).
Oleksynowa, K., Komornicki, T., 1996. Chemizm wód. In: Mirek, Z. (Ed.), Przyroda Tatrzańskiego Parku Narodowego. Tatrzański Park Narodowy, Kraków-Zakopane, pp. 197–214 (in polish).
Park, Y.S., Céréghino, R., Compin, A., Lek, S., 2003. Application of artificial neural networks for patterning and predicting aquatic insect species richness in running waters. Ecological Modelling 160, 265–280.
Peeters, L., Bação, F., Lobo, V., Dassargues, A., 2006. Exploratory data analysis and clustering of multivariate spatial hydrogeological data by means of GEO3DSOM, a variant of Kohonen's Self-Organizing Map. Hydrology and Earth System Sciences Discussions 3, 1487–1516.
PN-C-04638-02, 1989. Water and waste water, ion balance of water, method of calculation ion balance of water.
Rogalski, R., 1984. Badania znacznikowe przepływów podziemnych w Dolinie Chochołowskiej w Polskich Tatrach Zachodnich. Przegląd Geologiczny 32, 223–225 (in polish).
Sarkisian, N., 2008. Neural networks as an emergent method in quantitative research, an example of self-organiznig maps. In: Nagy Hesse-Biber, S., Leavy, P. (Eds.), Handobook of Emergent Methods. The Guilford Press, New York, USA, pp. 630–631.
Simeonov, V., Wolska, L., Kuczyncska, A., Gurwin, J., Tsakovski, S., Protasowicki, M., Namiesćnik, J., 2007. Sediment-quality assessment by intelligent data analysis. TrAC – Trends in Analytical Chemistry 26 (4), 323–331.
Skwarzec, B., Kabat, K., Astel, A., 2009. Seasonal and spatial variability of 210Po, 238U and 239+240Pu levels in the river catchment area assessed by application of neural-network based classification. Journal of Environmental Radioactivity 100 (2), 167–175.
Stanimirova, I., Połowniak, M., Skorek, R., Kita, A., John, E., Buhl, F., Walczak, B., 2007. Chemometric analysis of the water purification process data. Talanta 74 (10), 153–162.
Stuchlík, E., Kopáček, J., Fott, J., Hořická, Z., 2006. Chemical composition of the Tatra Mountain lakes: Response to acidification. Biologia, Section Zoology, Bratislava 61 (Suppl. 18), 11–20.
Trafas, K., 1985. Atlas Tatrzańskiego Parku Narodowego. TPN – PTPNoZ, Zakopane-Kraków, Poland (in polish).
Trepińska, J.B., 2004. Air temperature variability in the mountain areas based on Zakopane and Kasprowy Wierch examples. In: Haladyn, K., Mikłaszewski, A., Radomski, R., Ropuszyński, P. (Eds.), Climate–Environment–Human. Polish Ecological Club, Wrocław, Poland, pp. 33–40.
Tsakovski, S., Kudlak, B., Simeonov, V., Wolska, L., Namieśnik, J., 2009. Ecotoxicity and chemical sediment data classification by the use of self-organising maps. Analytica Chimica Acta 631 (2), 142–152.
Ultsch, A., Siemon, H.P., 1990. Kohonen's self organizing feature maps for exploratory data analysis. In: Proceedings of International Neural Network Conference (INNC'90). Kluwer, Dordrecht, The Netherlands, pp. 305–308.
Vesanto, J., 2000. Neural network tool data mining: SOM Toolbox. In: Proceedings of Symposium on Tool Environments and Development Methods for Intelligent Systems (TOOL-MET2000). Oulun yliopistopaino, Oulu, Finland, pp. 184–196.
Zhang, J., Dong, Y., Xi, Y., 2008. A comparison of SOFM ordination with DCA and PCA in gradient analysis of plant communities in the midst of Taihang Mountains, China. Ecological Informatics 3 (6), 367–374.
Żelazny, M., Kot, M., Rzonca, B., Siwek, J., 2007. Skład chemiczny wód w wybranych małych zlewniach w Dolinie Chochołowskiej w Tatrach. Współczesne Problemy Hydrogeologii 13, 919–928 (in polish).
Vesanto, J., Himberg, J., Alhoniemi, E., Parhankagas, J., 2000. SOM Toolbox for Matlab 5, Report A57. http://www.cis.hut.fi/projects/somtoolbox/.